Journal of Engineering and Sustainable Development
Vol. 29, No. 04, July 2025
https://jeasd.uomustansiriyah.edu.iq/index.php/jeasd
ISSN 2520-0917
Research Article
https://doi.org/10.31272/jeasd.2825

Voltage Control of 3-Phase 4-Leg Multilevel Inverter with Minimum Number of Switching States

Firas H. K. AL-Fadhli[1], Ammar Ibrahim Majeed[2], Mohammad Hameed Khazaal[3*], Benmessaoud Mohammed Tarik[4]

[1] Department of Research and Development, Ministry of Higher Education and Scientific Research, Baghdad, Iraq
[2] Department of Systems Engineering, College of Information Engineering, Al-Nahrain University, Baghdad, Iraq
[3] Defense Industries Commission, State Company for Military Industries, Al-Karama & Al-Harith Factory, Baghdad, Iraq
[4] Electrical and Electronics Engineering Faculty, University of Sciences and Technology of Oran, USTO-MB, Algeria

*Email: mohammadkhazaal1972@gmail.com

Article Info

Received 07/03/2024
Revised 27/03/2025
Accepted 16/05/2025

Abstract

This paper uses a finite control set (FCS) model predictive control (MPC) technique to control the output voltage of a 3-phase 4-leg multilevel inverter with a minimum number of switching states to supply a balanced, unbalanced, or nonlinear load. Good results are obtained when using this technique for a flying-capacitor (FC) multilevel inverter with an output that includes a filter made of capacitors and inductors. In this method, 19 switching states are used instead of 81 switching states in classical inverters, reducing the time required to reach the optimal solution in the cost function (g). The cost function calculates the minimum error between the output and reference voltage by selecting the optimal switching state for driving all inverter transistors. This technique can be applied to other types of multilevel inverters without considering the type of load used or needing to adjust the controller parameters. The inverter is designed for powering the 3-phase loads by separately generating three output voltages from the fourth leg using MPC.

Keywords: Cost function; Flying capacitor inverter; Model predictive control; Multilevel inverter; States reduction

1. Introduction

Three-phase inverters are the most important devices used in various applications, such as renewable energy systems, air conditioning systems, elevators, uninterruptible power supplies (UPS), planes, and electric vehicles, due to their ability to generate high power with high-quality output voltage with reduced harmonic distortion. To improve the quality of the output voltage waveform and increase power conversion efficiency for high-power applications, a multilevel inverter is preferred compared to a conventional inverter [1]-[4]. Compared with two-level inverters, three-phase three-leg multilevel inverters are usually preferred in medium and high-power applications because of their high-performance specifications such as low voltage stress, low switching losses, and low total harmonic distortion (THD) [3], [5]. The three-phase three-leg multilevel inverters are convenient for balanced loads as no current passes through their neutral point. As for unbalanced or nonlinear loads that cause unbalanced currents to flow in the loads [6], a path is needed for the zero-sequence current to flow through the neutral point to reduce its bad effect. Therefore, a fourth leg is added to the conventional three-phase inverter [7].

Generally, three types of three-phase three-leg multilevel inverters are used for high-power applications. Cascaded H-bridge inverter, Neutral-point clamped (NPC) inverter, and Flying-capacitor (FC) inverter. These topologies have advantages and disadvantages, which are discussed in [3]. These topologies have a common drawback: it is difficult to control the load voltage in case of an unbalanced or nonlinear load. There are multiple techniques used to control the conventional inverters, such as: pulse width modulation (PWM) [8]-[12] and three-dimensional space vector modulation (3-D SVM) [8], [13]-[15].

The 4-leg inverter is an enhancement of the conventional 3-leg inverter. The 3-phase, 4-leg inverter aims to keep the required sinusoidal waveform of the output voltage at all loading conditions and transients. This is perfect for applications like military equipment, communication devices, industrial automation, and all critical loads, which need outstanding performance UPS [16]. Also, the 4-leg multilevel inverter enhances the conventional 4-leg inverter. Presently, researchers worldwide are making great efforts to enhance the performance of these inverters, considering the control facilitation and the performance of the numerous optimization algorithms. Their goal is to increase power capability and improve the THD content of the sinusoidal waveform of the output voltage, the capacitor's voltage balancing of the DC link, and the load currents ripple. The disadvantage of the 4-leg multilevel inverters is an increase in the complexity of the control part under all load conditions [17]-[20], which has been overcome in this research.

Several techniques are used to control the output voltage of the multilevel inverter. PWM and SVPWM techniques are the two most famous techniques for controlling the voltage and current of the inverter. The SVPWM technique was initially invented as a vector approach of PWM for the 3-phase inverter to achieve maximum DC utilization. It is considered a complex technique that creates a sine wave to produce a higher voltage to the load with maximum DC utilization and lower THD. It marks a boundary space vector to be used according to the location of the output voltage vector.

Numerous modulation methods were used to control the output voltage of the multilevel inverter. Most of these methods try to control the output voltage from a specific point of view, such as minimizing THD, switching loss, response speed, and difficulty of algorithms [21]. Four fundamental modulation methods are used to produce the required sinusoidal pulse width modulation (SPWM) signal for driving multilevel inverters. These are [21], [22]: 1) phase disposition (PD) or in-phase disposition (IPD) at which every carrier signals are in phase; 2) phase opposition disposition (POD) in which every carrier signals below the zero reference are in opposition but above the zero reference are in phase, 3) alternative phase opposition disposition (APOD) where every carrier signals are alternatively in opposite disposition, and 4) phase shifted (PS) control technique. These methods are implemented as illustrated in Fig. 1. The first method (IPD) gives the best THD among all modulation methods [22]. The same methods can be used for producing the essential space vector pulse width modulation (SVPWM) signals for driving multilevel inverters as illustrated in Fig. 2 [21]-[23]. The MPC method is the third accurate and straightforward technique [24]-[30] used to achieve a sinusoidal output voltage with minimum THD. Also, the MPC was used to control the output current [31] voltage [24] for 3-phase, 4-leg NPC multilevel inverters using 16 transistors with 81 switching states. The number of switching states is huge, requiring much time to calculate and reach the optimal one. This paper uses only 19 switching states for a 3-phase, 4-leg FC inverter, which reduces the time required to calculate and reach the optimal switching state.

2. Classical 3-Phase 4-Leg 3-Level FC Inverter

A classical 3-phase, 4-leg, 3-level FC inverter with LC filter and NPC is illustrated in Fig. 3. The number of possible switching states (n_{states}) in a 3 3-phase, 4-leg, 3-level inverter is [32]- [35]:

$$n_{states} = 3^4 = 81\, States$$

To derive the multilevel inverter's mathematical model, the load voltages that depend on the switching states must be described in the building. The inverter switches are used to connect the inverter 3-phase terminal loads between the positive (P) point and the negative (N) point of the DC source (V_{dc}). The states S_1, S_2, S_3, S_4, S_5, S_6, S_7, and S_8 represent eight switching control commands, which create 81 switching states. Where $\overline{S_1}$, $\overline{S_2}$, $\overline{S_3}$, $\overline{S_4}$, $\overline{S_5}$, $\overline{S_6}$, $\overline{S_7}$ and $\overline{S_8}$ are the inverted of S_1, S_2, S_3, S_4, S_5, S_6, S_7 and S_8, respectively. These switching states are illustrated in Table 1, where (|Vi |) and (∠|Vi |°) are the magnitude and direction of the resultant vectors, respectively. Fig.3 has the LC filter with a balanced resistive load for simplicity, but this strategy can be implemented for unbalanced or nonlinear loads. The output voltages of the inverter (V_{an}, V_{bn}, and V_{cn}) for each phase can be written by using switching states as:

$$\begin{bmatrix} V_{an} \\ V_{bn} \\ V_{cn} \end{bmatrix} = \begin{bmatrix} (\mathrm{S_1} + \mathrm{S_2}) - (\mathrm{S_7} + \mathrm{S_8}) \\ (\mathrm{S_3} + \mathrm{S_4}) - (\mathrm{S_7} + \mathrm{S_8}) \\ (\mathrm{S_5} + \mathrm{S_6}) - (\mathrm{S_7} + \mathrm{S_8}) \end{bmatrix} \times 0.5\ \mathrm{V_{dc}} \qquad (1)$$

The following equations can be obtained for the circuit in Fig. 3 by applying Kirchhoff's voltage law:

$$\left.\begin{aligned} V_{an} &= R_1 i_{R1} + L_a \frac{di_a}{dt} \\ V_{bn} &= R_2 i_{R2} + L_b \frac{di_b}{dt} \\ V_{cn} &= R_3 i_{R3} + L_c \frac{di_c}{dt} \end{aligned}\right\} \qquad (2)$$

Where,

R_1, R_2, and R_3 are output resistive loads for phases a, b, and c.

L_a, L_b, and L_c are inductances of the filter for phases a, b, and c.

i_{R1}, i_{R2}, and i_{R3} are load currents for phases a, b, and c.

i_a, i_b, and i_c are inverter output currents.

Let,

$$\left.\begin{aligned} V_{oa} &= R_1 i_{R1} \\ V_{ob} &= R_2 i_{R2} \\ V_{oc} &= R_3 i_{R3} \end{aligned}\right\} \qquad (3)$$

Voa, Vob, and V_{ob} are the load voltages for phases a, b, and c.

Substitute (3) into (2) leads to:

$$\left.\begin{aligned} L_a \frac{di_a}{dt} &= V_{an} - V_{oa} \\ L_b \frac{di_b}{dt} &= V_{bn} - V_{ob} \\ L_c \frac{di_c}{dt} &= V_{cn} - V_{oc} \end{aligned}\right\} \qquad (4)$$

Using Kirchhoff's current law for the circuit of Fig.3 leads to:

$$\left.\begin{aligned} C_1\frac{dV_{oa}}{dt} &= i_a - i_{R1} \\ C_2\frac{dV_{ob}}{dt} &= i_b - i_{R2} \\ C_3\frac{dV_{oc}}{dt} &= i_c - i_{R3} \end{aligned}\right\} \tag{5}$$

C_1, C_2, and C_3 are capacitances of the filter for phases a, b, and c.

For simplicity, the inductance currents and load voltages can be expressed as vectors:

$$i_o = [i_a \;\; i_b \;\; i_c]^T \tag{6}$$

$$v_o = [V_{oa} \;\; V_{ob} \;\; V_{oc}]^T \tag{7}$$

and

$$R_f = [R_1 \;\; R_2 \;\; R_3]^T \tag{8}$$

$$L_f = [L_a \;\; L_b \;\; L_c]^T \tag{9}$$

$$C_f = [C_1 \;\; C_2 \;\; C_3]^T \tag{10}$$

$$V_n = [V_{an} \;\; V_{bn} \;\; V_{cn}]^T \tag{11}$$

$$i_R = [i_{R1} \;\; i_{R2} \;\; i_{R3}]^T \tag{12}$$

The neutral current is expressed as follows:

$$i_n = i_a + i_b + i_c \tag{13}$$

Equations (4) and (5) can be expressed as a state space in continuous time:

$$\dot{x}(t) = Ax(t) + Bu(t) \tag{14}$$

Where,

$$\dot{x}(t) = \frac{dx}{dt} \tag{15}$$

$$x(t) = \begin{bmatrix} i_o \\ v_o \end{bmatrix} \tag{16}$$

$$A = \begin{bmatrix} 0 & \frac{-1}{L_f} \\ \frac{1}{C_f} & 0 \end{bmatrix} \tag{17}$$

$$B = \begin{bmatrix} \frac{1}{L_f} & 0 \\ 0 & \frac{-1}{C_f} \end{bmatrix} \tag{18}$$

$$u(t) = \begin{bmatrix} V_n \\ i_R \end{bmatrix} \tag{19}$$

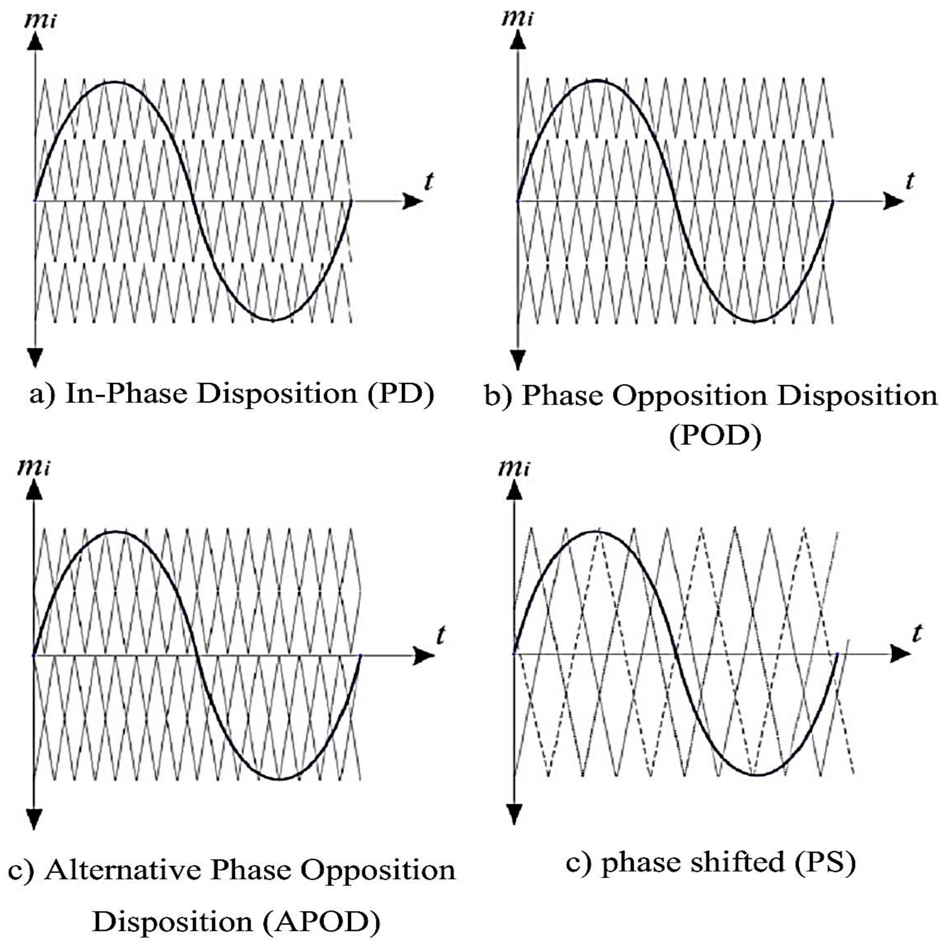

Figure 1. Modulation control methods for SPWM.

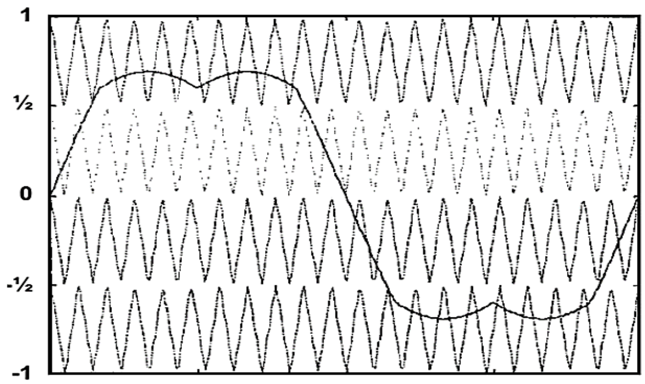

Figure 2. In-phase disposition (IPD) control method for SVPWM.

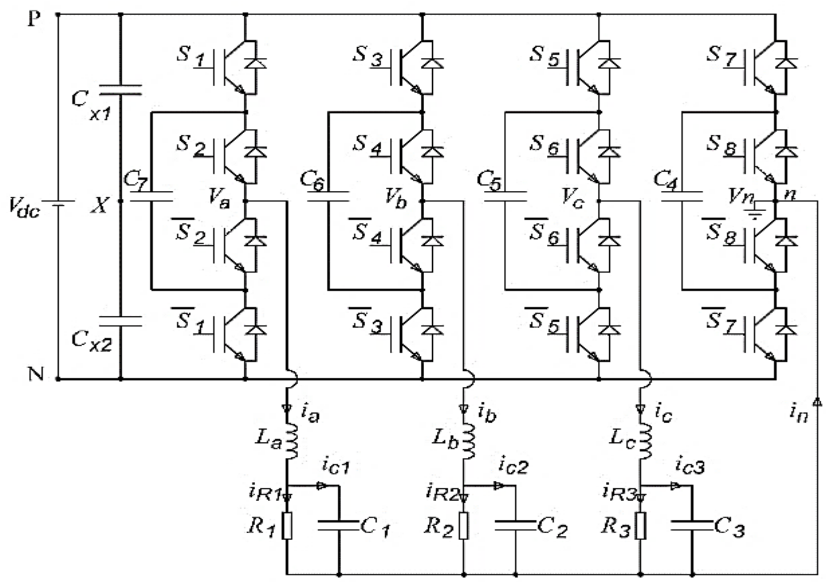

Figure 3. 3-phase, 4-leg FC inverters with LC filter.

Table 1. Switching states of 3-phase, 4-leg FC inverters.

Voltage vectors	S_1	S_2	S_3	S_4	S_5	S_6	S_7	S_8	V_{an}	V_{bn}	V_{cn}	$\|V_i\|$	$\angle\|V_i\|°$
V_1	0	0	0	0	0	0	0	0	0	0	0	0	0
V_2	0	1	0	1	0	1	0	0	0.5	0.5	0.5	0	0
V_3	1	1	1	1	1	1	0	0	1	1	1	0	0
V_4	1	1	0	1	0	1	0	0	1	0.5	0.5	0.5	0
V_5	0	1	0	0	0	0	0	0	0.5	0	0	0.5	0
V_6	0	1	0	1	0	0	0	0	0.5	0.5	0	0.5	60
V_7	1	1	1	1	0	1	0	0	1	1	0.5	0.5	60
V_8	0	1	1	1	0	1	0	0	0.5	1	0.5	0.5	120
V_9	0	0	0	1	0	0	0	0	0	0.5	0	0.5	120
V_{10}	0	1	1	1	1	1	0	0	0.5	1	1	0.5	180
V_{11}	0	0	0	1	0	1	0	0	0	0.5	0.5	0.5	180
V_{12}	0	1	0	1	1	1	0	0	0.5	0.5	1	0.5	-120
V_{13}	0	0	0	0	0	1	0	0	0	0	0.5	0.5	-120
V_{14}	1	1	0	1	1	1	0	0	1	0.5	1	0.5	-60
V_{15}	0	1	0	0	0	1	0	0	0.5	0	0.5	0.5	-60
V_{16}	1	1	0	0	0	0	0	0	1	0	0	1	0
V_{17}	1	1	0	1	0	0	0	0	1	0.5	0	0.86	30
V_{18}	1	1	1	1	0	0	0	0	1	1	0	1	60
V_{19}	0	1	1	1	0	0	0	0	0.5	1	0	0.86	90
V_{20}	0	0	1	1	0	0	0	0	0	1	0	1	120
V_{21}	0	0	1	1	0	1	0	0	0	1	0.5	0.86	150
V_{22}	0	0	1	1	1	1	0	0	0	1	1	1	180
V_{23}	0	0	0	1	1	1	0	0	0	0.5	1	0.86	-150
V_{24}	0	0	0	0	1	1	0	0	0	0	1	1	-120
V_{25}	0	1	0	0	1	1	0	0	0.5	0	1	0.86	-90
V_{26}	1	1	0	0	1	1	0	0	1	0	1	1	-60
V_{27}	1	1	0	0	0	1	0	0	1	0	0.5	0.86	-30
V_{28}	0	0	0	0	0	0	0	1	-0.5	-0.5	-0.5	0	0
V_{29}	0	1	0	1	0	1	0	1	0	0	0	0	0
V_{30}	1	1	1	1	1	1	0	1	0.5	0.5	0.5	0	0
V_{31}	1	1	0	1	0	1	0	1	0.5	0	0	0.5	0
V_{32}	0	1	0	0	0	0	0	1	0	-0.5	-0.5	0.5	0
V_{33}	0	1	0	1	0	0	0	1	0	0	-0.5	0.5	60
V_{34}	1	1	1	1	0	1	0	1	0.5	0.5	0	0.5	60
V_{35}	0	1	1	1	0	1	0	1	0	0.5	0	0.5	120
V_{36}	0	0	0	1	0	0	0	1	-0.5	0	-0.5	0.5	120
V_{37}	0	1	1	1	1	1	0	1	0	0.5	0.5	0.5	180
V_{38}	0	0	0	1	0	1	0	1	-0.5	0	0	0.5	180
V_{39}	0	1	0	1	1	1	0	1	0	0	0.5	0.5	-120
V_{40}	0	0	0	0	0	1	0	1	-0.5	-0.5	0	0.5	-120
V_{41}	1	1	0	1	1	1	0	1	0.5	0	0.5	0.5	-60
V_{42}	0	1	0	0	0	1	0	1	0	-0.5	0	0.5	-60
V_{43}	1	1	0	0	0	0	0	1	0.5	-0.5	-0.5	1	0

Table 1. (continued)

Voltage vectors	S_1	S_2	S_3	S_4	S_5	S_6	S_7	S_8	V_{an}	V_{bn}	V_{cn}	$\lvert V_i \rvert$	$\angle \lvert V_i \rvert °$
V_{44}	1	1	0	1	0	0	0	1	0.5	0	-0.5	0.866	30
V_{45}	1	1	1	1	0	0	0	1	0.5	0.5	-0.5	1	60
V_{46}	0	1	1	1	0	0	0	1	0	0.5	-0.5	0.866	90
V_{47}	0	0	1	1	0	0	0	1	-0.5	0.5	-0.5	1	120
V_{48}	0	0	1	1	0	1	0	1	-0.5	0.5	0	0.866	150
V_{49}	0	0	1	1	1	1	0	1	-0.5	0.5	0.5	1	180
V_{50}	0	0	0	1	1	1	0	1	-0.5	0	0.5	0.866	-150
V_{51}	0	0	0	0	1	1	0	1	-0.5	-0.5	0.5	1	-120
V_{52}	0	1	0	0	1	1	0	1	0	-0.5	0.5	0.866	-90
V_{53}	1	1	0	0	1	1	0	1	0.5	-0.5	0.5	1	-60
V_{54}	1	1	0	0	0	1	0	1	0.5	-0.5	0	0.866	-30
V_{55}	0	0	0	0	0	0	1	1	-1	-1	-1	0	0
V_{56}	0	1	0	1	0	1	1	1	-0.5	-0.5	-0.5	0	0
V_{57}	1	1	1	1	1	1	1	1	0	0	0	0	0
V_{58}	1	1	0	1	0	1	1	1	0	-0.5	-0.5	0.5	0
V_{59}	0	1	0	0	0	0	1	1	-0.5	-1	-1	0.5	0
V_{60}	0	1	0	1	0	0	1	1	-0.5	-0.5	-1	0.5	60
V_{61}	1	1	1	1	0	1	1	1	0	0	-0.5	0.5	60
V_{62}	0	1	1	1	0	1	1	1	-0.5	0	-0.5	0.5	120
V_{63}	0	0	0	1	0	0	1	1	-1	-0.5	-1	0.5	120
V_{64}	0	1	1	1	1	1	1	1	-0.5	0	0	0.5	180
V_{65}	0	0	0	1	0	1	1	1	-1	-0.5	-0.5	0.5	-180
V_{66}	0	1	0	1	1	1	1	1	-0.5	-0.5	0	0.5	-120
V_{67}	0	0	0	0	0	1	1	1	-1	-1	-0.5	0.5	-120
V_{68}	1	1	0	1	1	1	1	1	0	-0.5	0	0.5	-60
V_{69}	0	1	0	0	0	1	1	1	-0.5	-1	-0.5	0.5	-60
V_{70}	1	1	0	0	0	0	1	1	0	-1	-1	1	0
V_{71}	1	1	0	1	0	0	1	1	0	-0.5	-1	0.866	30
V_{72}	1	1	1	1	0	0	1	1	0	0	-1	1	60
V_{73}	0	1	1	1	0	0	1	1	-0.5	0	-1	0.866	90
V_{74}	0	0	1	1	0	0	1	1	-1	0	-1	1	120
V_{75}	0	0	1	1	0	1	1	1	-1	0	-0.5	0.866	150
V_{76}	0	0	1	1	1	1	1	1	-1	0	0	1	180
V_{77}	0	0	0	1	1	1	1	1	-1	-0.5	0	0.866	-150
V_{78}	0	0	0	0	1	1	1	1	-1	-1	0	1	-120
V_{79}	0	1	0	0	1	1	1	1	-0.5	-1	0	0.866	-90
V_{80}	1	1	0	0	1	1	1	1	0	-1	0	1	-60
V_{81}	1	1	0	0	0	1	1	1	0	-1	-0.5	0.866	-30

The model discretization is accomplished using the Euler forward approximation for all equations having derivatives, which gives satisfactory accuracy [36] - [39].

$$\frac{dV_{oa}}{dt} = \frac{V_{oa}(k+1)-V_{oa}(k)}{T_s} \tag{20}$$

Where T_s is the sampling period. The predicted load voltages can be obtained by substituting (20) in (5):

$$\left.\begin{aligned} V_{oa}(k+1) &= \frac{T_s}{C_1} i_a(k) - \frac{T_s}{C_1} i_{R1}(k) + V_{oa}(k) \\ V_{ob}(k+1) &= \frac{T_s}{C_2} i_b(k) - \frac{T_s}{C_2} i_{R2}(k) + V_{ob}(k) \\ V_{oc}(k+1) &= \frac{T_s}{C_3} i_c(k) - \frac{T_s}{C_3} i_{R3}(k) + V_{oc}(k) \end{aligned}\right\} \tag{21}$$

In order to predict the load voltages (21), the load currents must be calculated. So, the load currents can be estimated by rewriting (21) as:

$$\left.\begin{aligned} i_{R1}(k\text{-}1) &= i_a(k\text{-}1)\text{-}\frac{C_1}{T_s}\left(V_{oa}(k)\text{-}V_{oa}(k\text{-}1)\right) \\ i_{R2}(k\text{-}1) &= i_b(k\text{-}1)\text{-}\frac{C_2}{T_s}\left(V_{ob}(k)\text{-}V_{ob}(k\text{-}1)\right) \\ i_{R3}(k\text{-}1) &= i_c(k\text{-}1)\text{-}\frac{C_3}{T_s}\left(V_{oa}(k)\text{-}V_{oc}(k\text{-}1)\right) \end{aligned}\right\} \quad (22)$$

Equation (21) illustrates that predicting the load's predictive voltage at the instant $(k+1)$ requires measuring the load voltages (V_{oa}, V_{ob}, and V_{oc}), load currents (i_{R1}, i_{R2}, and i_{R3}), and inductance currents (i_a, i_b, and i_c). The load voltage depends on the inverter output voltage (V_{an}, V_{bn}, and V_{cn}), which depends on the DC source and switching signals according to (1). Fig. 4 illustrates the block diagram of the FCS-MPC system.

3. Minimizing the Number of Switching States

As explained earlier in Table 1, the 3-level, 4-leg FC inverter usually uses 81 switching states, which is a large number. This will increase the time required to reach the optimal solution for choosing the optimal switching state. In this paper, the proposed strategy is to use only 19 switching states to drive the FC multilevel inverter.

Table 1 can be rearranged according to the magnitude of the vectors ($|V_i|$) and direction ($\angle|V_i|°$) as shown in Table 2. The voltage vectors are plotted according to the complex numbers shown in Fig.5. (Projection in two dimensions) representing the vertices of the 24 triangles, which represent big tetrahedrons, and these tetrahedrons consist of small tetrahedra [40]-[42]. Table 2 consists of 19 groups of vectors of equal value in magnitude ($|V_i|$) and direction ($\angle|V_i|°$). If grouped into 19 states, each state from each group will achieve the same desired purpose. Therefore, Table 2 can be minimized into 19 switching states as shown in Table 3. Therefore, this strategy decreases the cost function (g) calculation process for minimizing the error between the reference of the load voltages and the calculated prediction of the load voltages at the instant $(k+1)$. Fig. 6 shows a flow chart of the voltage control FCS-MPC algorithm.

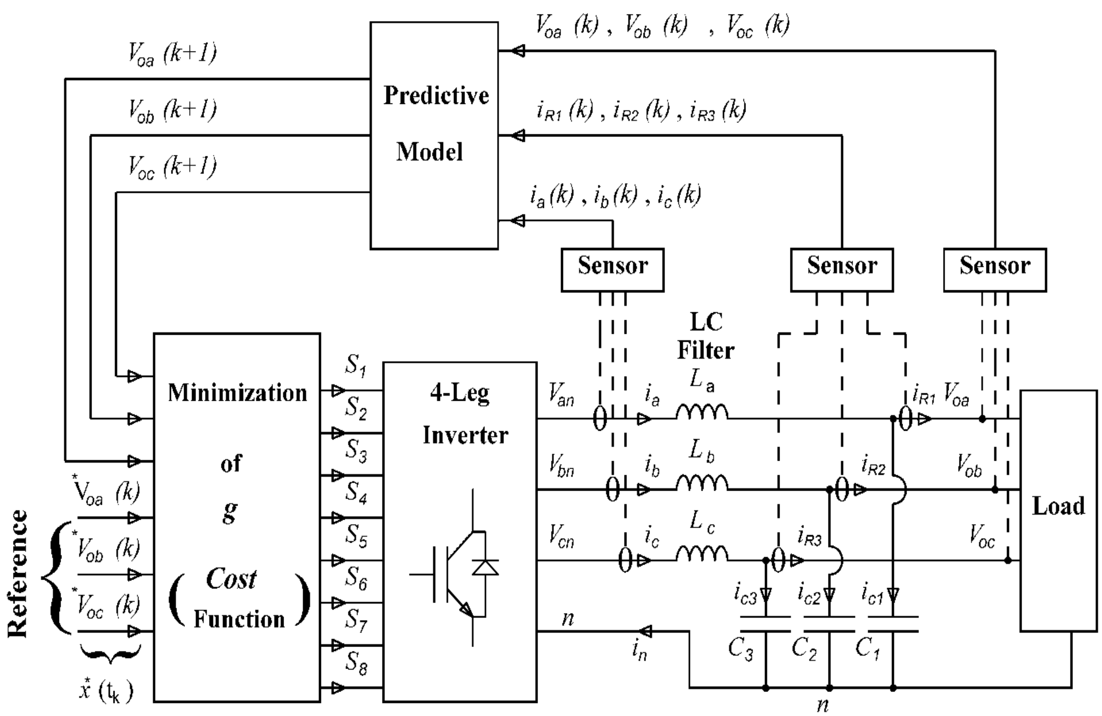

Figure 4. FCS-MPC control block diagram.

Table 2. Switching state of 3-phase, 4-leg FC inverter.

Voltage vectors	S_1	S_2	S_3	S_4	S_5	S_6	S_7	S_8	V_{an}	V_{bn}	V_{cn}	$\lvert V_i \rvert$	$\angle \lvert V_i \rvert°$	Groups
V_1	0	0	0	0	0	0	0	0	0	0	0	0	0	
V_2	0	1	0	1	0	1	0	0	0.5	0.5	0.5	0	0	
V_3	1	1	1	1	1	1	0	0	1	1	1	0	0	
V_{28}	0	0	0	0	0	0	0	1	-0.5	-0.5	-0.5	0	0	
V_{29}	0	1	0	1	0	1	0	1	0	0	0	0	0	1
V_{30}	1	1	1	1	1	1	0	1	0.5	0.5	0.5	0	0	
V_{55}	0	0	0	0	0	0	1	1	-1	-1	-1	0	0	
V_{56}	0	1	0	1	0	1	1	1	-0.5	-0.5	-0.5	0	0	
V_{57}	1	1	1	1	1	1	1	1	0	0	0	0	0	
V_4	1	1	0	1	0	1	0	0	1	0.5	0.5	0.5	0	
V_5	0	1	0	0	0	0	0	0	0.5	0	0	0.5	0	
V_{31}	1	1	0	1	0	1	0	1	0.5	0	0	0.5	0	2
V_{32}	0	1	0	0	0	0	0	1	0	-0.5	-0.5	0.5	0	
V_{58}	1	1	0	1	0	1	1	1	0	-0.5	-0.5	0.5	0	
V_{59}	0	1	0	0	0	0	1	1	-0.5	-1	-1	0.5	0	
V_6	0	1	0	1	0	0	0	0	0.5	0.5	0	0.5	60	
V_7	1	1	1	1	0	1	0	0	1	1	0.5	0.5	60	
V_{33}	0	1	0	1	0	0	0	1	0	0	-0.5	0.5	60	3
V_{34}	1	1	1	1	0	1	0	1	0.5	0.5	0	0.5	60	
V_{60}	0	1	0	1	0	0	1	1	-0.5	-0.5	-1	0.5	60	
V_{61}	1	1	1	1	0	1	1	1	0	0	-0.5	0.5	60	
V_8	0	1	1	1	0	1	0	0	0.5	1	0.5	0.5	120	4
V_9	0	0	0	1	0	0	0	0	0	0.5	0	0.5	120	
V_{35}	0	1	1	1	0	1	0	1	0	0.5	0	0.5	120	
V_{36}	0	0	0	1	0	0	0	1	-0.5	0	-0.5	0.5	120	
V_{62}	0	1	1	1	0	1	1	1	-0.5	0	-0.5	0.5	120	
V_{63}	0	0	0	1	0	0	1	1	-1	-0.5	-1	0.5	120	
V_{10}	0	1	1	1	1	1	0	0	0.5	1	1	0.5	180	
V_{11}	0	0	0	1	0	1	0	0	0	0.5	0.5	0.5	180	
V_{37}	0	1	1	1	1	1	0	1	0	0.5	0.5	0.5	180	5
V_{38}	0	0	0	1	0	1	0	1	-0.5	0	0	0.5	180	
V_{64}	0	1	1	1	1	1	1	1	-0.5	0	0	0.5	180	
V_{65}	0	0	0	1	0	1	1	1	-1	-0.5	-0.5	0.5	-180	
V_{12}	0	1	0	1	1	1	0	0	0.5	0.5	1	0.5	-120	
V_{13}	0	0	0	0	0	1	0	0	0	0	0.5	0.5	-120	
V_{39}	0	1	0	1	1	1	0	1	0	0	0.5	0.5	-120	6
V_{40}	0	0	0	0	0	1	0	1	-0.5	-0.5	0	0.5	-120	
V_{66}	0	1	0	1	1	1	1	1	-0.5	-0.5	0	0.5	-120	
V_{67}	0	0	0	0	0	1	1	1	-1	-1	-0.5	0.5	-120	
V_{14}	1	1	0	1	1	1	0	0	1	0.5	1	0.5	-60	
V_{15}	0	1	0	0	0	1	0	0	0.5	0	0.5	0.5	-60	
V_{41}	1	1	0	1	1	1	0	1	0.5	0	0.5	0.5	-60	7
V_{42}	0	1	0	0	0	1	0	1	0	-0.5	0	0.5	-60	
V_{68}	1	1	0	1	1	1	1	1	0	-0.5	0	0.5	-60	
V_{69}	0	1	0	0	0	1	1	1	-0.5	-1	-0.5	0.5	-60	
V_{17}	1	1	0	1	0	0	0	0	1	0.5	0	0.866	30	
V_{44}	1	1	0	1	0	0	0	1	0.5	0	-0.5	0.866	30	8
V_{71}	1	1	0	1	0	0	1	1	0	-0.5	-1	0.866	30	
V_{19}	0	1	1	1	0	0	0	0	0.5	1	0	0.866	90	
V_{46}	0	1	1	1	0	0	0	1	0	0.5	-0.5	0.866	90	9
V_{73}	0	1	1	1	0	0	1	1	-0.5	0	-1	0.866	90	
V_{21}	0	0	1	1	0	1	0	0	0	1	0.5	0.866	150	10

Table 2. (continued).

Voltage vectors	S_1	S_2	S_3	S_4	S_5	S_6	S_7	S_8	V_{an}	V_{bn}	V_{cn}	$\|V_i\|$	$\angle\|V_i\|°$	Groups
V_{48}	0	0	1	1	0	1	0	1	-0.5	0.5	0	0.866	150	
V_{75}	0	0	1	1	0	1	1	1	-1	0	-0.5	0.866	150	
V_{23}	0	0	0	1	1	1	0	0	0	0.5	1	0.866	-150	
V_{77}	0	0	0	1	1	1	1	1	-1	-0.5	0	0.866	-150	11
V_{50}	0	0	0	1	1	1	0	1	-0.5	0	0.5	0.866	-150	
V_{25}	0	1	0	0	1	1	0	0	0.5	0	1	0.866	-90	
V_{52}	0	1	0	0	1	1	0	1	0	-0.5	0.5	0.866	-90	12
V_{79}	0	1	0	0	1	1	1	1	-0.5	-1	0	0.866	-90	
V_{27}	1	1	0	0	0	1	0	0	1	0	0.5	0.866	-30	
V_{54}	1	1	0	0	0	1	0	1	0.5	-0.5	0	0.866	-30	13
V_{81}	1	1	0	0	0	1	1	1	0	-1	-0.5	0.866	-30	
V_{70}	1	1	0	0	0	0	1	1	0	-1	-1	1	0	
V_{43}	1	1	0	0	0	0	0	1	0.5	-0.5	-0.5	1	0	14
V_{16}	1	1	0	0	0	0	0	0	1	0	0	1	0	
V_{72}	1	1	1	1	0	0	1	1	0	0	-1	1	60	
V_{18}	1	1	1	1	0	0	0	0	1	1	0	1	60	15
V_{45}	1	1	1	1	0	0	0	1	0.5	0.5	-0.5	1	60	
V_{74}	0	0	1	1	0	0	1	1	-1	0	-1	1	120	
V_{20}	0	0	1	1	0	0	0	0	0	1	0	1	120	16
V_{47}	0	0	1	1	0	0	0	1	-0.5	0.5	-0.5	1	120	
V_{76}	0	0	1	1	1	1	1	1	-1	0	0	1	180	
V_{49}	0	0	1	1	1	1	0	1	-0.5	0.5	0.5	1	180	17
V_{22}	0	0	1	1	1	1	0	0	0	1	1	1	180	
V_{78}	0	0	0	0	1	1	1	1	-1	-1	0	1	-120	
V_{51}	0	0	0	0	1	1	0	1	-0.5	-0.5	0.5	1	-120	18
V_{24}	0	0	0	0	1	1	0	0	0	0	1	1	-120	
V_{80}	1	1	0	0	1	1	1	1	0	-1	0	1	-60	
V_{26}	1	1	0	0	1	1	0	0	1	0	1	1	-60	19
V_{53}	1	1	0	0	1	1	0	1	0.5	-0.5	0.5	1	-60	

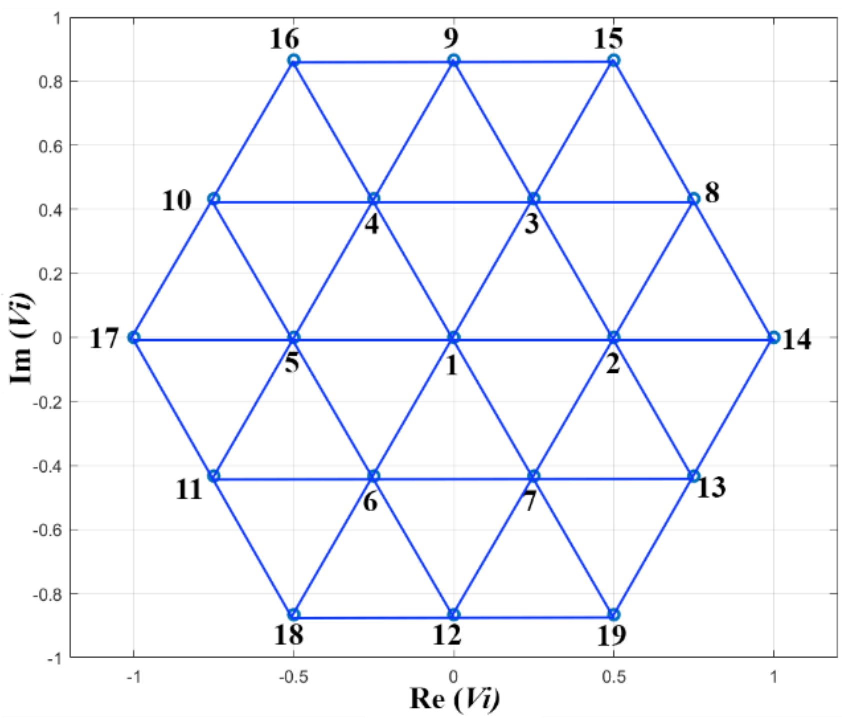

Figure 5. Projection of voltage vectors according to the complex numbers.

Table 3. Proposed switching state of 3-phase, 4-leg FC inverter.

Voltage vectors	S_1	S_2	S_3	S_4	S_5	S_6	S_7	S_8	V_{an}	V_{bn}	V_{cn}	$\lvert V_i \rvert$	$\angle\lvert V_i \rvert°$	Groups
V_1	0	0	0	0	0	0	0	0	0	0	0	0	0	1
V_4	1	1	0	1	0	1	0	0	1	0.5	0.5	0.5	0	2
V_6	0	1	0	1	0	0	0	0	0.5	0.5	0	0.5	60	3
V_8	0	1	1	1	0	1	0	0	0.5	1	0.5	0.5	120	4
V_{10}	0	1	1	1	1	1	0	0	0.5	1	1	0.5	180	5
V_{12}	0	1	0	1	1	1	0	0	0.5	0.5	1	0.5	-120	6
V_{14}	1	1	0	1	1	1	0	0	1	0.5	1	0.5	-120	7
V_{17}	1	1	0	1	0	0	0	0	1	0.5	0	0.866	30	8
V_{19}	0	1	1	1	0	0	0	0	0.5	1	0	0.866	90	9
V_{21}	0	0	1	1	0	1	0	0	0	1	0.5	0.866	150	10
V_{23}	0	0	0	1	1	1	0	0	0	0.5	1	0.866	-150	11
V_{25}	0	1	0	0	1	1	0	0	0.5	0	1	0.866	-90	12
V_{27}	1	1	0	0	0	1	0	0	1	0	0.5	0.866	-30	13
V_{70}	1	1	0	0	0	0	1	1	0	-1	-1	1	0	14
V_{72}	1	1	1	1	0	0	1	1	0	0	-1	1	60	15
V_{74}	0	0	1	1	0	0	1	1	-1	0	-1	1	120	16
V_{76}	0	0	1	1	1	1	1	1	-1	0	0	1	180	17
V_{78}	0	0	0	0	1	1	1	1	-1	-1	0	1	-120	18
V_{80}	1	1	0	0	1	1	1	1	0	-1	0	1	-60	19

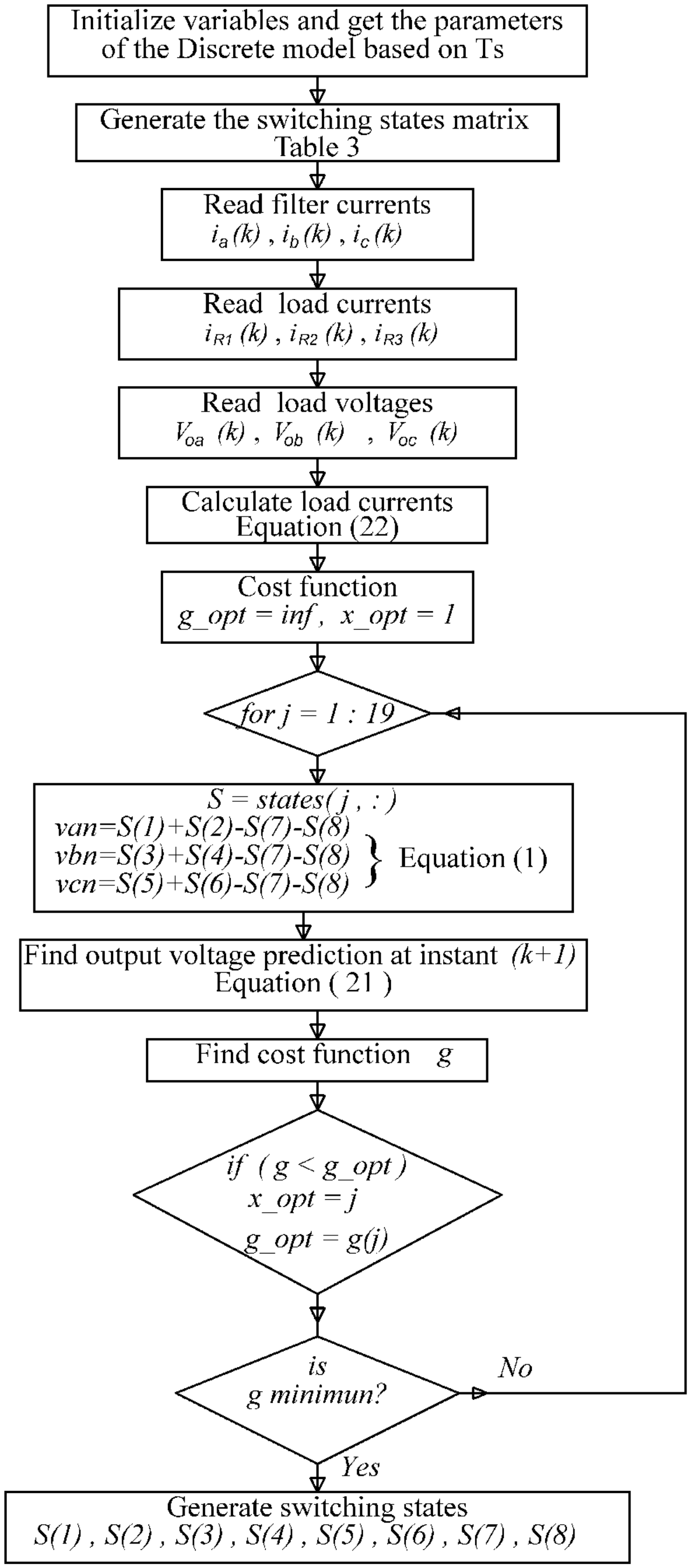

Figure 6. Flowchart of the proposed predictive control algorithm.

4. Simulation of FCS-MPC Voltage Control with Cost Function Optimization

A Simulink MATLAB model is carried out using an FCS-MPC voltage controller for a 3-phase, 4-leg FC inverter as illustrated in Fig.7. The inputs of the Simulink MATLAB model controller (MPC) are the load voltages (V_{oa}, V_{ob}, and V_{oc}), inductance currents (i_a, i_b, and i_c), the DC input voltage of the inverter (V_{dc}), three reference voltages, and inductances and capacitors of the inverter filter. In contrast, load currents (i_{R1}, i_{R2}, and i_{R3}) are calculated in this model according to (22). According to (21), the MPC model produces eight drive signals (S_1, S_2, S_3, S_4, S_5, S_6, S_7, and S_8) for driving the power stage of the inverter (Subsystem 1 of Fig. 8).

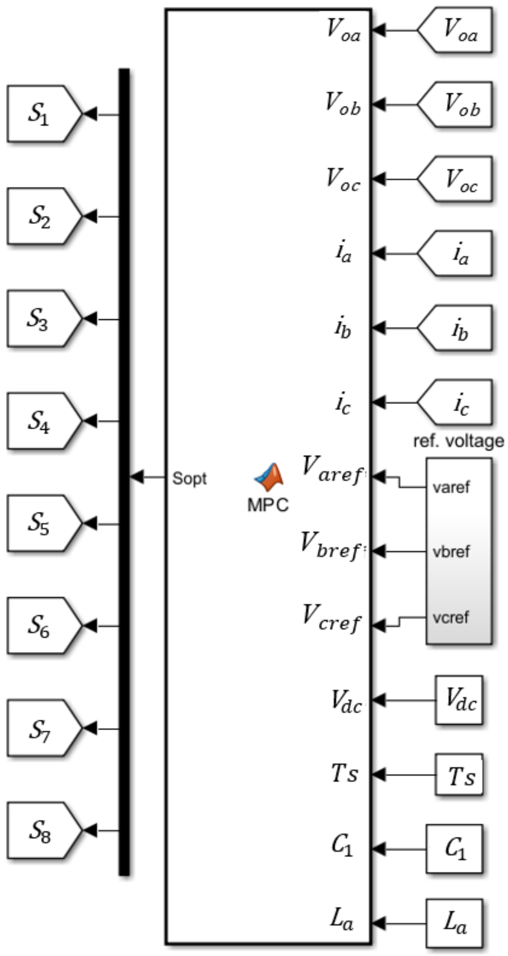

Figure 7. Simulink MATLAB model controller (FCS-MPC voltage control) for 3-phase, 4-leg FC multilevel inverter.

Fig. 8 represents the Simulink MATLAB model for the power stage of the multilevel inverter with LC filter and load. The types of load of the inverter are shown in Fig.9. The system parameters used in the Simulink MATLAB model simulation, such as the inverter's DC input voltage, reference voltages, sampling time, switching frequency, flying capacitance, and LC filter, are shown in Table 4. The load characteristics used in the simulation are given in Table 5, which includes 5 cases of the load conditions.

Fig. 10 to 14 show the load voltages, load currents, and neutral currents under the five load conditions. The load voltage figures show that the FCS-MPC controller can regulate the load voltage with low harmonic distortion for all 5 cases of load conditions.

The load voltages are sinusoidal and close to the reference voltage with a minimum THD. Fig. 15 to Fig. 19 represent the THD for the output voltage of phase (a) for all 5 cases of load conditions, which shows that the THD is not more than 2.59%, occurring with a nonlinear unbalanced load (Fig.19).

From all results, the 4-leg inverter creates independent regulated voltages for each leg and thus helps to control the neutral current (zero sequence current). The load voltages track their reference voltages very well.

Table 4. System parameters.

Parameters	Values
DC input voltage of the inverter	$V_{dc} = 500V$
Reference voltages	$V_{aref} = V_{bref} = V_{cref} = 200\text{V}$
Sampling time	$Ts = 1\mu s$
Switching frequency	$fs = 50\text{kHz}$
Flying capacitance	$C_4 = C_5 = C_6 = C_7 = 220\mu f$
LC filter	$C_1 = C_2 = C_3 = 20\mu f$ $L_a = L_b = L_c = 20mH$

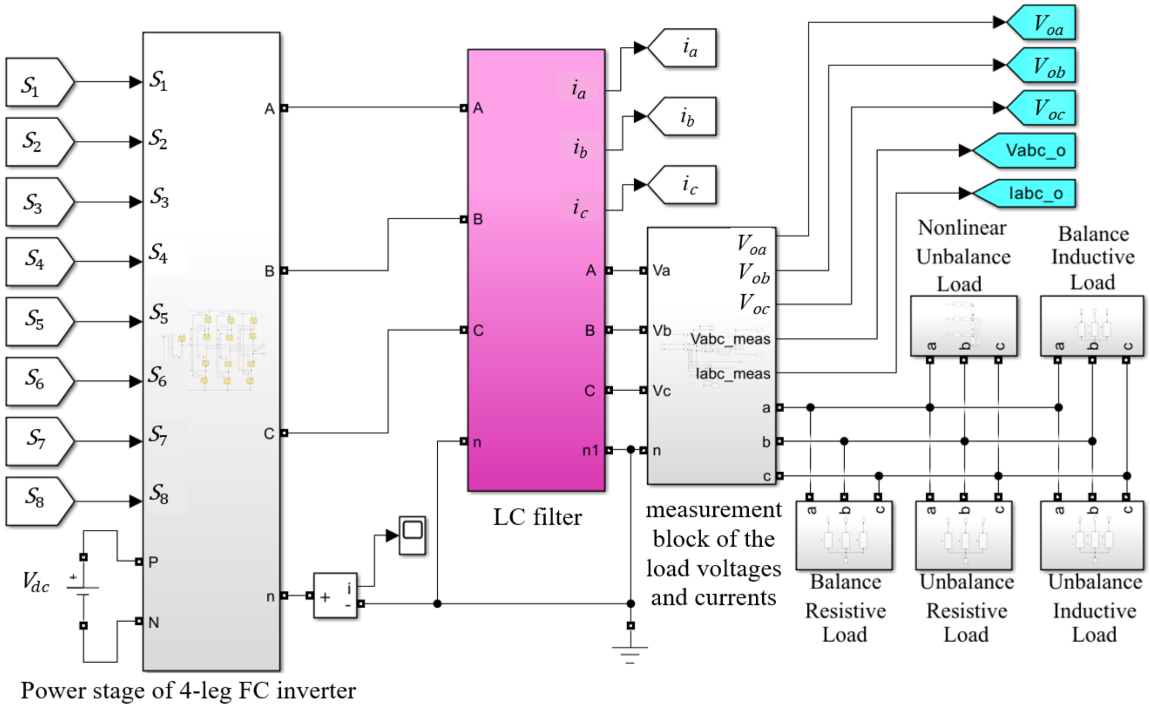

Figure 8. Simulink MATLAB model for power stage with LC filter and load.

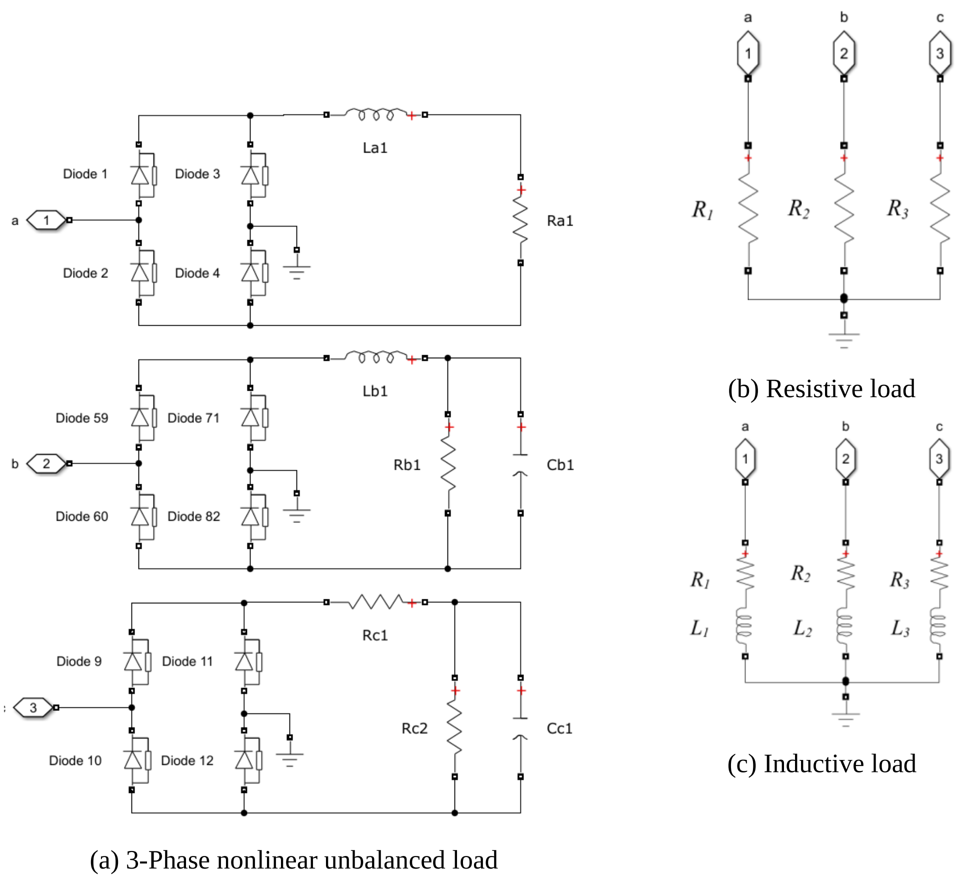

Figure 9. Types of load of the inverter.

Table 5. Load characteristics of the inverter operated at reference voltages.

No.	Type of load	Case of load	Load values
1	Resistive	Balance	$R_1 = R_2 = R_3 = 50\Omega$
2	Resistive	unbalance	$R_1 = 90\Omega, R_2 = 50\Omega, R_3 = 20\Omega$
3	Inductive	Balance	$R_1 = R_2 = R_3 = 20\Omega$ $L_1 = L_2 = L_3 = 15mH$
4	Inductive	unbalance	$R_1 = 90\Omega, R_2 = 50\Omega, R_3 = 20\Omega$ $L_1 = 50mH, L_2 = 100mH, L_3 = 150mH$
5	Nonlinear	unbalance	$R_{a1} = 20\Omega, L_{a1} = 40mH$ $R_{b1} = 5\Omega, R_{b2} = 60\Omega, C_{b1} = 2000\mu f$ $R_{c1} = 80\Omega, L_{b1} = 30mH, C_{b1} = 4000\mu f$

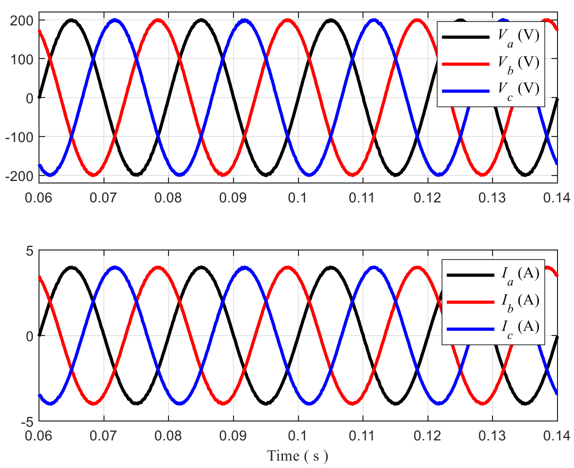

Figure 10: Output voltages and currents of the FC inverter under balanced resistive load.

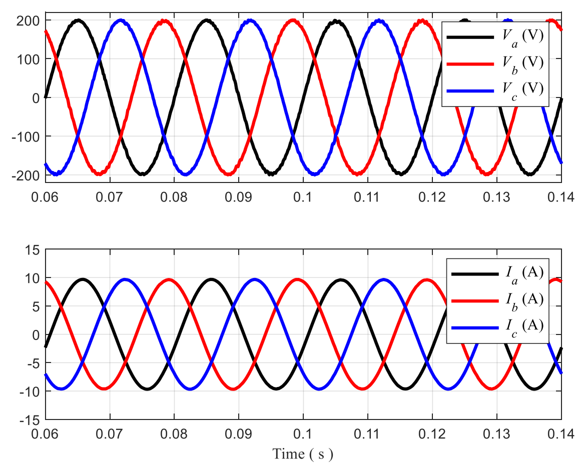

Figure 12. Output voltages and currents of the FC inverter under a balanced inductive load.

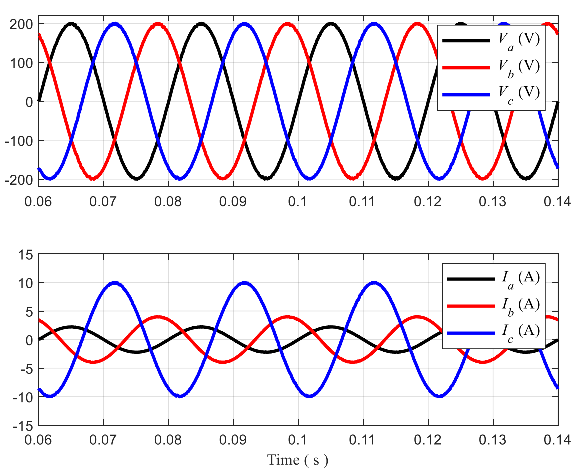

Figure 11. Output voltages and currents of the FC inverter under unbalanced resistive load.

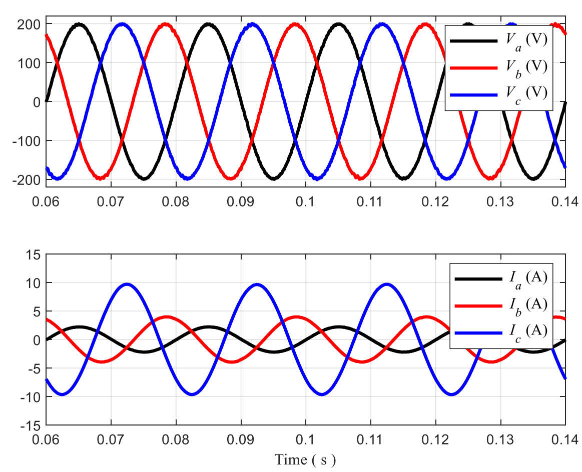

Figure 13. Output voltages and currents of the FC inverter under an unbalanced inductive load.

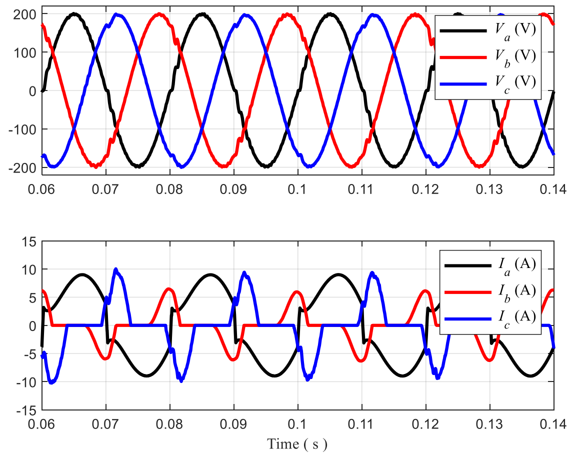

Figure 14. Output voltages and currents of the FC inverter under nonlinear unbalanced load.

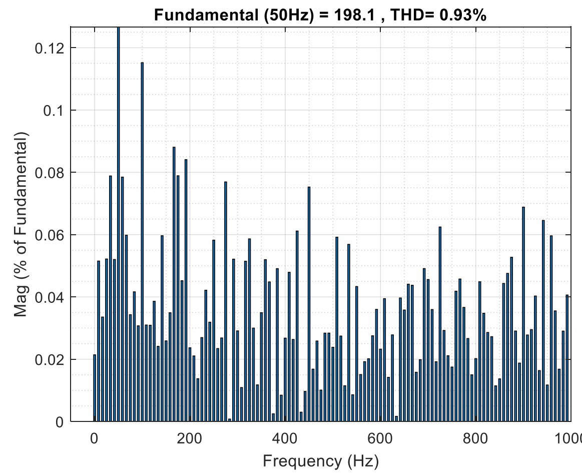

Figure 17. THD of the FC inverter output voltage under a balanced inductive load.

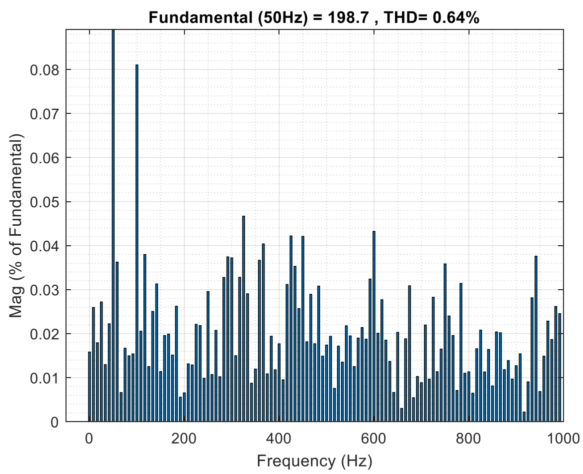

Figure 15. THD of the FC inverter output voltage under balanced resistive load.

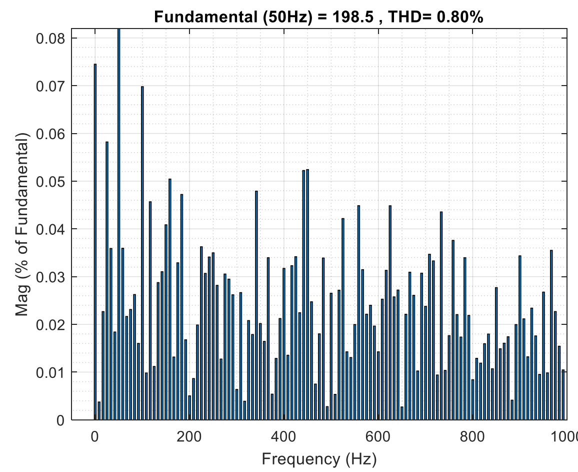

Figure 18. THD of the FC inverter output voltage under an unbalanced inductive load.

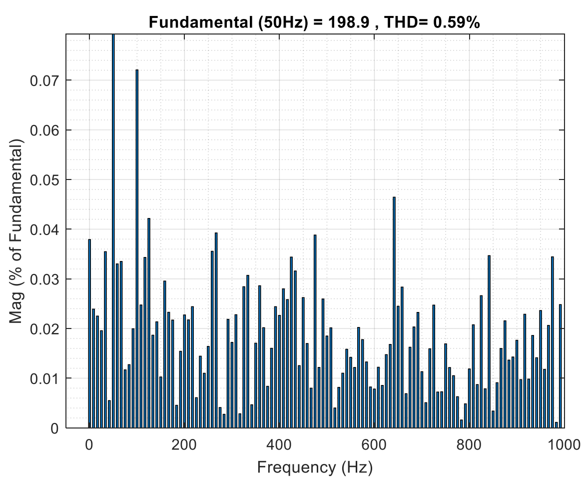

Figure 16. THD of the FC inverter output voltage under unbalanced resistive load.

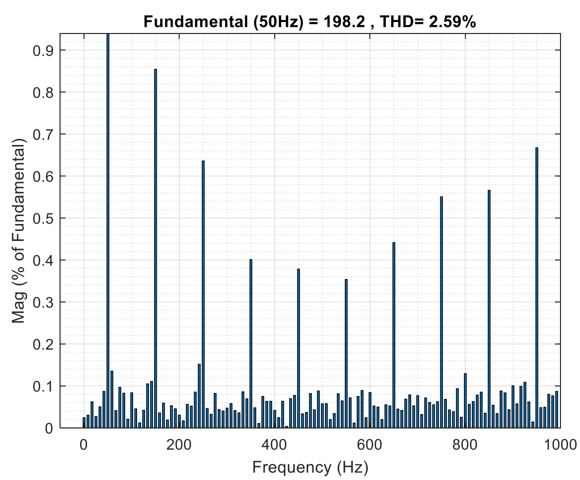

Figure 19. THD of the FC inverter output voltage under nonlinear unbalanced load.

5. Conclusion

The FCS-MPC voltage controller for 3-phase, 4-leg FC multilevel inverters is modeled and simulated using MATLAB/Simulink with minimum switching state. During the design and modeling of the multilevel inverters, the main problem is the complexity of achieving a regulated voltage under unbalanced or nonlinear loads with many levels and switching states (81), which requires a long time to reach the optimal switching state. This problem is solved using the FCS-MPC voltage controller with only 19 switching states. The gate drives of transistors are directly produced from the FCS-MPC controller without any modulator. This method is easy, very efficient, and suitable for inverters without considering the type of load used and without needing to adjust the parameters. Also, this type of controller can be used with high-level inverters without significant modifications to the controller. According to the results obtained from the MATLAB/Simulink, regulated output voltages were obtained with a sine wave having a few harmonics under all 5 cases of load conditions in the steady state mode. These features make the FCS-MPC algorithm a perfect choice for design and implementation.

Acknowledgment

The researchers would like to extend their sincere thanks to the departments in which they work and the administrations in charge of them for providing the appropriate work environment and offering financial and moral support throughout work on the current research.

Conflict of Interest

The authors declare that there are no conflicts of interest regarding the publication of this manuscript.

Author Contribution Statement

Firas Al-Fadhli collected data, investigated, and prepared software. Ammar Ibrahim performed system simulation and proposed and programmed the selected control method. Mohammad Hameed performed result analysis, prepared the original draft, supervised, reviewed work, and validated; all authors approved the final version.

References

[1] T. Bertin, G. Despesse, and R. Thomas, “Comparison between a cascaded h-bridge and a conventional h-bridge for a 5-kw grid-tied solar inverter,” Electronics, vol. 12, no. 8, Apr. 2023, Art. No. 1929, doi: https://doi.org/10.3390/electronics12081929

[2] H. Aws Al-Jrew, R. Jawad Mahmood, and S. Ramzy Ali, “Comparison of new multilevel inverter topology with conventional topologies used for induction heating system,” IJEEE, vol. 18, no. 1, pp. 48-57, Jun. 2022, doi: https://doi.org/10.37917/ijeee.18.1.6

[3] A. Balal, S. Dinkhah, F. Shahabi, M. Herrera, and Y. Lung Chuang, “A review on multilevel inverter topologies,” Emerging Science Journal, vol. 6, no. 1, pp. 185-200, Feb. 2022, doi: https://doi.org/10.28991/ESJ-2022-06-01-014

[4] K. Jena, D. Kumar, K. Janardhan, B. Kumar, A. Singh, S. Nikolovski and M. Bajaj, “A novel three-phase switched-capacitor five-level multilevel inverter with reduced components and self-balancing ability,” Applied Sciences, vol 13, no. 3, pp. 1-19, Jan. 2023, doi: https://doi.org/10.3390/app13031713

[5] U. Chourasia and P. Tiwari, “Comparative analysis of two-level, three-level, five-level, and seven-level H bridge inverter,” IRJET, vol. 7, no. 12, pp. 444-449, Dec. 2020, https://www.irjet.net/archives/V7/i12/IRJET-V7I1277.pdf

[6] John J. Grainger, William D. Stevenson, “Power system analysis,” McGraw-Hill, Inc., 1st edition, 2021.

[7] I. Abdulbaqi, A. Ahmed, R. Omar, and A. Abdulsada, “Modeling and analysis of a four-leg inverter using space vector pulse width modulation technique,” JEASD, vol. 23, no. 2, pp. 100-119, Mar. 2019, doi: https://doi.org/10.31272/jeasd.23.2.9

[8] R. Aboelsaud, A. Ibrahim, A. Garganeev, “Review of three-phase inverters control for unbalanced load compensation,” IJPEDS, vol. 10, no. 1, pp. 242-255, Mar. 2019, doi: https://doi.org/10.11591/ijpeds.v10.i1.pp242-255

[9] A. Garganeev, R. Aboelsaud, and A. Ibrahim, “Voltage control of autonomous three-phase four-leg VSI based on scalar PR controllers,” 20th International Conference of Young Specialists on Micro/Nanotechnologies and Electron Devices (EDM), pp. 558-564. Sep. 2019, doi: https://doi.org/10.1109/EDM.2019.8823098

[10] C. Roh, H. Jeon, S. Kim, J. Kim, N. Lee, and S. Song, “Optimal hybrid pulse width modulation for three-phase inverters in electric propulsion ships,” Machines, vol. 12, no. 2, pp. 1-19. Feb. 2024, doi: https://doi.org/10.3390/machines12020109

[11] L. Fangke, L. Haifeng, L. Yongdong, and C. Jianyun, “A modulation method to eliminate common-mode voltage of dual three-phase motor,” IEEE Transportation Electrification Conference and Expo (ITEC), pp. 1-5, Aug. 2019, doi: https://doi.org/10.1109/ITEC.2019.8790480

[12] A. Poorfakhraei, M. Narimani, A. Emadi, “A Review of Modulation and Control Techniques for Multilevel Inverters in Traction Applications,” IEEE Access, vol. 9, pp. 24187-24204. Feb. 2021, doi: https://doi.org/10.1109/ACCESS.2021.3056612

[13] C. Santhakumar, C. Bharatiraja, K. Gowrishankar, K.M. Ravi Eswar and J. Vinoth, “Extended over modulation zone three-dimensional SVPWM for three-level neutral-point-clamped,” Materials Today: Proceedings, vol. 52, Part 3, pp. 1756-1762, Feb. 2022, doi: https://doi.org/10.1109/ACCESS.2021.3056612

[14] D. Tran and N. Nguyen, “SVPWM strategies to reduce common-mode voltage for five-level ANPC inverter,” AETA 2022—Recent Advances in Electrical Engineering and Related Sciences: Theory and Application, vol. 1081, pp. 371-384, 2024, doi: https://doi.org/10.1109/ACCESS.2021.3056612

[15] B. Yu, W. Song and Y. Guo, “A simplified and generalized SVPWM scheme for two-level multiphase inverters with common-mode voltage reduction,” IEEE Transactions on Industrial Electronics, vol. 69, no. 2, pp. 1378-1388, Feb. 2022, doi: https://doi.org/10.1109/TIE.2021.3063966

[16] M. Fraser, C. Manning, and B. Wells, “Transformerless four-wire PWM rectifier and its application in AC-DC-AC converters,” IEEE Proceedings - Electric Power Applications, vol. 142, no. 6, pp. 410-416, Nov. 1995, doi: https://doi.org/10.1049/ip-epa:19952278.

[17] A. Mustafa, “Multilevel inverters using finite set- model predictive current control for renewable energy systems applications,” Ph.D. Thesis, Cape Peninsula University of Technology. 2015, Article link: http://hdl.handle.net/20.500.11838/1202

[18] A. Lewicki, M. Morawiec, “Control strategy for the multilevel cascaded H-bridge converter,” International Conference-Workshop Compatibility and Power Electronics, pp. 310-315, Sep. 2013, doi: https://doi.org/10.1109/CPE.2013.6601175

[19] G. Srinivasan, M. Rivera, V. Loganathan, D. Ravikumar, and B. Mohandip, “Trends and Challenges in Multilevel Inverters with Reduced Switches,” Energies, vol. 10, no. 4, pp. 368-391, Feb. 2021, doi: https://doi.org/10.3390/electronics10040368

[20] J. Rodríguez, J. Lai, and F. Peng, “Multilevel Inverters: A Survey of Topologies, Controls, and Applications,” IEEE Transactions on Industrial Electronics, vol. 49, no.4, pp. 724 -738, Aug. 2002, doi: https://doi.org/10.1109/TIE.2002.801052

[21] F. AL-Fadhli and M. Khazaal, “Design and simulation of a multilevel inverter with Scott connection transformer based on STATCOM using low frequency modulation,” AIP Conference Proceedings 2386, 040010, vol. 2386, no. 1, Jan. 2022, doi: https://doi.org/10.1063/5.0067063

[22] B. Wu, M. Narimani, “High-Power Converters and AC Drives,” John Wiley & Sons, Inc., 2nd edition, 2006. https://ieeexplore.ieee.org/servlet/opac?bknumber=7823162.

[23] G. Carrara, S. Gardella, M. Marchesoni, R. Salutari, and G. Sciutto, “A new multilevel PWM method: a theoretical analysis,” IEEE Transactions on Power Electronics, vol. 7, no. 3, pp. 497-505, Jul. 1992, doi: https://doi.org/10.1109/63.145137

[24] Q. Al-Attwani, “Model predictive control of a four-leg three-phase inverter,” M.Sc. Thesis, Urmia University, Urmia, Iran, 2024.

[25] Y. Chen and M. Laza, “An efficient MPC algorithm for switched systems with minimum dwell time constraints,” Automatica, vol. 143, pp. 110453, Sep. 2022, doi: https://doi.org/10.1016/j.automatica.2022.110453.

[26] S. Zaid, I. Mohamed, A. Bakeer, L. Liu, H. Albalawi, M. Tawfiq, and A. Kassem, “From MPC-Based to End-to-End (E2E) Learning-Based Control Policy for Grid-Tied 3L-NPC Transformerless Inverter,” IEEE Access, vol. 10, pp. 57309 - 57326, May. 2022, doi: https://doi.org/10.1109/ACCESS.2022.3173752

[27] A. Kumar, G. Kumar, D. Sreenivasarao and H. Myneni, “Model predictive current control of DSTATCOM with simplified weighting factor selection using VIKOR method for power quality improvement,” IET Generation, Transmission & Distribution, vol 13, no. 16, pp. 33649-3660, Jul. 2019, doi: https://doi.org/10.1049/iet-gtd.2018.6782

[28] A. Castro, “Optimal Switching Sequence Model Predictive Control for Power Electronics,” Ph.D. Thesis, Universidad De Chile, 2019.

[29] L. Kang, J. Cheng, B. Hu, X. Luo, and J. Zhang, “A Simplified Optimal-Switching-Sequence MPC with Finite-Control-Set Moving Horizon Optimization for Grid-Connected Inverter,” ADPT electronics, vol. 8, no. 4, pp. 457, Apr. 2019, doi: https://doi.org/10.3390/electronics8040457.

[30] F. Donoso, A. Mora, R. Cardenas, A. Angulo, D. Saez, and M. Rivera, “Finite-set model-predictive control strategies for a 3L-NPC inverter operating with fixed switching frequency,” IEEE Transactions on Industrial Electronics, vol. 65, no. 5, pp. 3954 - 3965, May 2018, doi: https://doi.org/10.1109/TIE.2017.2760840.

[31] V. Yaramasu, M. Rivera, M. Narimani, B. Wu, and J. Rodriguez, “Finite State Model-based Predictive Current Control with Two-step Horizon for Four-leg NPC Converters,” Journal of Power Electronics, vol. 14, no. 6, pp. 1178-1188, 2014, doi: https://doi.org/10.6113/JPE.2014.14.6.1178

[32] C. Roh, “Performance Comparisons of Three-Phase/Four-Wire Model Predictive Control-Based DC/AC Inverters Capable of Asymmetric Operation for Wave Energy Converters,” ADPI Energies, vol. 15, no. 8, pp. 2839-2860, Apr. 2022, doi: https://doi.org/10.3390/en15082839.

[33] N. Dai, M. Wong, and Y. Han, “Application of a Three-level NPC Inverter as a Three-Phase Four-Wire Power Quality Compensator by Generalized 3DSVM,” IEEE Transactions on Power Electronics, vol. 21, no. 2, pp. 440-449, Mar. 2006, doi: https://doi.org/10.1109/TPEL.2005.8697552

[34] S. Mohapatra and V. Agarwal, “An Improved Reduced Complexity Model Predictive Current Controller for Grid Connected Four-Leg Multilevel Inverter,” IEEE Transactions on Industry Applications, vol. 56, no. 1, pp. 498-506, Jan. 2020, doi: https://doi.org/10.1109/TIA.2019.2952530

[35] P. Ramasamy and V. Krishnasamy, “A 3D-Space Vector Modulation Algorithm for Three Phase Four Wire Neutral Point Clamped Inverter Systems as Power Quality Compensator,” Energies, vol. 10, no.11, pp. 1792-1800, Nov. 2017, doi: https://doi.org/10.3390/en10111792

[36] V. Yaramasu, M. Rivera, B. Wu and J. Rodriguez, “Model Predictive Current Control of Two-Level Four-Leg Inverters - Part I: Concept, Algorithm and Simulation Analysis,” IEEE Transactions on Power Electronics, vol. 28, no. 7, pp. 3459-3468, Nov. 2013, doi: https://doi.org/10.1109/TPEL.2012.2227509

[37] M. Rivera, V. Yaramasu, J. Rodriguez and B. Wu, “Model Predictive Current Control of Two-Level Four-Leg Inverters - Part II: Experimental Implementation and Validation,” IEEE Transactions on Power Electronics, vol. 28, no. 7, pp. 3469-3478, Nov. 2013, doi: https://doi.org/10.1109/TPEL.2012.222782

[38] V. Yaramasu, M. Rivera, M. Narimani, B. Wu and J. Rodriguez, “Model Predictive Approach for a Simple and Effective Load Voltage Control of Four-Leg Inverter with an Output LC Filter,” IEEE Transactions on Industrial Electronics, vol. 61, no. 10, pp. 5259-5270, Jan. 2014, doi: https://doi.org/10.1109/TIE.2013.2297291

[39] M. Rivera, F. Morales, C. Baier, J. Munoz, L. Tarisciotti, P. Zanchetta, and P. Wheeler, “A Modulated Model Predictive Control Scheme for a Two-Level Voltage Source Inverter,” IEEE International Conference on Industrial Technology (ICIT), pp. 2224-2229, Mar. 2015, doi: https://doi.org/10.1109/ICIT.2015.7125425

[40] M. Fadel, A. Llor, B. Tran and A. Ziani, “Direct control of 4-Leg 4-Level Flying Capacitor Converter for an Active Filtering Application,” IFAC Proceedings Volumes, vol. 45, no. 21, pp. 325-330, Mar. 2013, doi: https://doi.org/10.3182/20120902-4-FR-2032.00058

[41] J. Morales, D. Gaona, M. Ángeles, R. Alzola and J. Zavala, “An Active Power Filter Based on a Three-Level Inverter and 3D-SVPWM for Selective Harmonic and Reactive Compensation,” Energies, vol. 10, no. 3, pp. 297-320, Mar. 2017, doi: https://doi.org/10.3390/en10030297

[42] A. Mohamed A. Baiju and M. Baiju, “A Novel Space Vector PWM Scheme for Multilevel Inverters,” Twenty-Fourth Annual IEEE Applied Power Electronics Conference and Exposition, pp. 671-676, Mar. 2009, doi: https://doi.org/10.1109/APEC.2009.4802732.